Framework coordination of single-ion Cu2+sites in hydrated 17O-ZSM-5 zeolite

Framework coordination of single-ion Cu^{2+} sites in hydrated ^{17}O-ZSM-5 zeolite

Arianna Actis[1], Enrico Salvadori[1,*], Mario Chiesa[1]

[1]Department of Chemistry and NIS Centre, University of Torino, Via Giuria 7, 10125 Torino (Italy)

Keywords: Zeolite; ZSM-5; single-ion site; interfacial coordination chemistry; oxygen-17; ENDOR

Abstract

Single metal ion sites supported on zeolites are an interesting topic both in basic research and in applied, heterogeneous catalysis. It is often assumed that the zeolite serves as a mere support useful to size-select reactants and products but that does not affect the chemistry of the metal ion, given the ionic nature of the chemical bond. In this work, single-ion Cu^{2+} sites are prepared in ZSM-5 through oxidation of the corresponding Cu^{+} species introduced via gas phase reaction, and then hydrated. Pulsed ENDOR and HYSCORE spectroscopies together with selective ^{17}O isotopic labelling of the oxide ions, either as framework oxygen or belonging to solvating water, are used to gain an atomistic structural description of the paramagnetic species formed at the interface and an insight into the properties of the Cu-O bonds. We prove that single-ion Cu^{2+} sites adopt a square planar coordination geometry, maintain a strong interaction with the zeolite framework even in presence of solvating water molecules and that all Cu-O bonds have a non-negligible covalent character. Further, we compare the hyperfine data obtained for Cu^{2+}-^{17}O with VO^{2+}-^{17}O and Zn^{+}-^{17}O and rationalise the observed trends within the framework of crystal field theory providing useful criteria for the interpretation of hyperfine data. The level of detail afforded by ^{17}O labelling and EPR techniques is remarkable in the understanding of the interfacial coordination chemistry of single-ion sites stabilised by zeolites.

1. Introduction

The labyrinthine network of channels and cages in zeolites, a class of well-defined crystalline aluminosilicates composed of corner sharing SiO_4 and AlO_4 tetrahedra, provides an ideal platform for the stabilization of single (transition) metal ions which, in these systems, often display unusual coordination and oxidation states. The substitution of aluminium (formally Al^{3+}) in place of silicon (Si^{4+}) in such frameworks produces a net negative charge, which stabilizes single metal sites. In principle, such isolated single metal sites catalysts mimic enzymatic analogues and show distinctive performances for a wide variety of chemical reactions.[1]

Single metal sites are therefore distinct entities defined by the coordination of the metal ion by the framework which acts both as a ligand and as support.[2] Under anhydrous conditions these sites are usually under coordinated and act as acidic Lewis centres. Ligating molecules such as water, often present in reaction mixtures, saturate the coordination sphere of the metal leading to solvated-like species with a high degree of mobility. Understanding the chemical bonding of single metal sites in the presence of solvating water molecules is therefore of critical importance in order to underpin structure-function relationships familiar to inorganic and organometallic homogeneous catalysis and improve catalytic efficiency by design.

Cu exchanged zeolites have been in the focus since the 1970s for their activity in selective catalytic reduction of nitrogen oxides[3,4] and they remain of interest in particular in the context of CH_4/CH_3OH and CH_3OH /propylene conversion[5,6]. In all these applications paramagnetic Cu^{2+} species are involved, which are amenable to electron paramagnetic resonance (EPR) studies[7,8]. Cu-zeolite catalysts are usually prepared by exchange in solution with Cu^{2+} salts, often leading to excessively copper-exchanged systems, containing mixtures of different Cu species. An alternative route to obtain well defined single metal sites is the reaction of the dehydrated zeolite framework with volatile molecular precursors.[9,10] In particular, CuCl has been shown to be particularly well suited to generate clean, isolated single sites, suitable for detailed spectroscopic

studies. Upon diffusion inside the zeolite channels, CuCl reacts with the most acidic Brönsted sites following the reaction reported in Figure 1[9]:

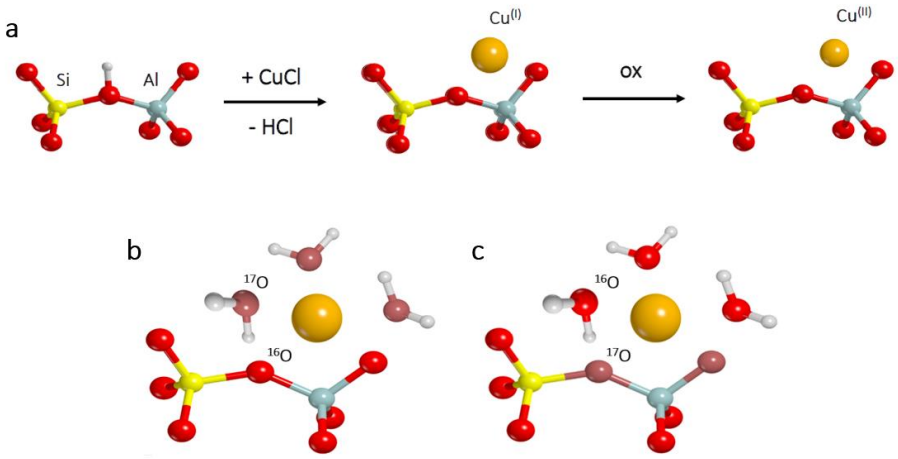

Figure 1. (a) Schematic representation of the protocol employed to synthetize single-ion Cu^{2+} sites in ZSM-5. The reduction in the ionic radius of copper upon oxidation is also illustrated. (b) and (c) graphical rendering of the samples considered in this study with either the solvating water molecules (b) or the zeolite framework (c) selectively labelled with ^{17}O. For clarity, in all panels only a portion of the ZSM-5 framework is shown. Colour code: Yellow: Silicon; Grey: Aluminium; Orange: Copper; White: Hydrogen; Red: Oxygen-16; Maroon: Oxygen-17.

In this way isolated and well-defined Cu^{+} (d^{10}, S = 0) sites are obtained, which can be converted to Cu^{2+} (d^{9}, S = 1/2) by direct oxidation.

Isotopic enrichment with ^{17}O (I = 5/2) of the Si-O-Al Brønsted motif provides a selective handle to investigate the nature of the Cu-O chemical bond with the framework oxide ions, if the magnetic interaction between the electron and nuclear magnetic moments can be detected. This can be achieved through measurements able to probe the hyperfine interaction between the metal electron spin and the ^{17}O nuclear spin. These experiments, termed Electron Nuclear DOuble Resonance (ENDOR)[11] and HYperfine Sublevel COrRElation (HYSCORE)[12] spectroscopies, yield the NMR spectrum of the paramagnetic centre thus marrying the selectivity of EPR towards the paramagnetic active centre and the exquisite chemical detail and resolution of NMR. Hyperfine couplings are strongly dependent on bond lengths and angles and can therefore be employed to define geometry and structure of interfacial coordination complexes with exquisite detail not easily achievable by other spectroscopies.

In this work through independent ^{17}O enrichment of either water molecules or the zeolite framework, we fully assess the coordination environment of a single Cu^{2+} metal site to conclude that it retains an intimate bonding with the zeolite framework even in the presence of solvating water molecules. Moreover, through comparisons with results on 1st row transition metal ions with complementary electronic structures – that is VO^{2+} ($3d^{1}$)[10] and Zn^{+} ($4s^{1}3d^{10}$)[13] - we establish the ^{17}O hyperfine coupling as a faithful reporter of the bonding interaction of paramagnetic single metal sites in interfacial coordination chemistry and we provide guidelines for the interpretation of ^{17}O hyperfine couplings within the framework of the crystal field theory.

2. Experimental section

2.1 Zeolite activation. Commercial H-ZSM5 (Zeolyst, Si/Al = 40) was dehydrated by thermal treatment under dynamic vacuum at 673 K for 2 h, followed by calcination for 1 h at 773 K in O_2 atmosphere to remove water and other impurities.

2.2 Copper exchange. Copper deposition was performed through gas-phase reaction between the activated support and CuCl vapors. [14] CuCl (Sigma-Aldrich, ReagentPlus, purity ≥ 99%) was introduced at the bottom of a cylindrical quartz tube that can be fitted to a high vacuum apparatus (residual pressure $1 \cdot 10^{-3}$ mbar) and covered with a fiber glass separator onto which the zeolite powder was placed. This apparatus was assembled in the glove box to ensure anhydrous conditions and to avoid spontaneous CuCl oxidation. The system was then heated at 573 K for 30 minutes, keeping it under dynamic vacuum, to allow CuCl sublimation, while at the same time eliminating the reaction side-product (HCl). After the treatment, the copper exchanged powder was transferred inside a glove box from the reaction vessel into a quartz cell equipped with an EPR tube. As prepared Cu^{+}-ZSM5 was subsequently oxidized to Cu^{2+}-ZSM5 by heating it at 348 K for 30 minutes in O_2 atmosphere.

2.3 ^{17}O enrichment of zeolite framework. Isotopic exchange of H-ZSM5 was obtained before copper deposition: the activated H-ZSM5 was contacted with $H_2{}^{17}O$ vapor (90% ^{17}O enrichment, Cambridge Isotope Laboratories, Inc.) and heated for 2 h at 393 K[13]. The sample was subsequently reacted with CuCl vapors as described in 2.2.

2.4 Hydration. Once performed copper exchange in anhydrous conditions, hydrated samples were obtained by exposing Cu^{2+}-ZSM5 to 20mbar vapors of H_2O or $H_2{}^{17}O$ (90% ^{17}O enrichment, Cambridge Isotope Laboratories, Inc.).

2.5 X-band CW EPR. X-band (microwave frequency 9.45 MHz) CW EPR measurements were performed on a Bruker EMX spectrometer equipped with a ER 4122 SHQ cylindrical cavity. A modulation frequency of 100 kHz, a modulation amplitude of 0.5 mT, and a microwave power of 1 mW (for spectra at 77 K) and of 10 mW (for spectra at room temperature) were used.

2.6 Q-band CW and Pulse EPR. Q-band (microwave frequency 33.7 GHz) CW EPR experiments were performed on a Bruker Elexys E580 spectrometer equipped with an EN 5107D2 Bruker resonator, an Oxford Instruments CF935 helium-flow cryostat and ITC503 temperature controller. Q-band electron-spin-echo (ESE) detected EPR spectra were recorded with the pulse sequence π/2−τ−π−τ−echo. Pulse lengths $t_{\pi/2}$ = 16 ns and t_{π} = 32 ns, a τ value of 200 ns was used.

2.7 ENDOR spectroscopy. Q-band Davies ENDOR spectra were recorded with both Mims and Davies pulse sequences. Davies ENDOR used the pulse sequence π-T- π/2- τ- π-τ-echo with π = 31 ns and π/2 = 16 ns, π_{RF} = 14 μs, T = 16 μs and τ = 200 ns. The use of unselective microwave pulses suppresses the small hyperfine couplings in favour of large ones. The spectra cover a radiofrequency range from 1 to 61 MHz with a resolution of 0.249 MHz, so that both ^{1}H and ^{17}O resonances could be detected at once (Figure 3). Q-band Mims ENDOR allowed a greater resolution of the weak ^{1}H hyperfine couplings and employed the pulse sequence π/2-τ-π/2- π_{RF} - π/2-τ-echo with π/2 = 16 ns, τ = 150 ns, π_{RF} = 14 μs and additional waiting times of 1 μs were used before and after the π_{RF} pulse. Mims ENDOR spectra were recorded in a 15 MHz window centered at the ^{1}H Larmor frequency, with a 0.043 MHz spectral resolution.

2.7.1 ^{1}H ENDOR. The high-frequency part of the spectrum is occupied by resonance signals due to weakly coupled ^{1}H nuclei, i.e. the hyperfine coupling is lower than the nuclear Zeeman interaction. Such signals are centered at the ^{1}H Larmor frequency (between 42 and 55 MHz depending on the field position) and with the two components separated by the hyperfine coupling constant ν_{ENDOR} = (ν_L (^{1}H) /h $\pm$A/h).

2.7.2 ^{17}O ENDOR. The low-frequency portion of the spectrum, between 2 and 40 MHz is attributed to strongly coupled (i.e. hyperfine larger than Zeeman interaction) ^{17}O nuclei. The resonance condition obeys

the relationship $\nu_{ENDOR} = A/2h \pm 2\nu_L(^{17}O)/h$ (assuming that the nuclear quadrupole contribution, which is not resolved in the experimental spectra, can be ignored).

2.8 HYSCORE spectroscopy. Q-band Hyperfine Sublevel Correlation (HYSCORE) spectroscopy experiments were carried out with the standard pulse sequence $\pi/2$-τ-$\pi/2$-t1-π-t2-$\pi/2$-τ-echo, applying an eight-step phase cycle for eliminating unwanted echoes. Microwave pulse lengths $\pi/2$ = 16 ns, π = 32 ns, and a shot repetition rate of 1.0 kHz were used. The t1 and t2 time intervals were incremented in steps of 8 or 16 ns, starting from 150 ns giving a data matrix of either 200 x 200 or 300 x 300 points, depending on the sample and field position. The time traces of the HYSCORE spectra were baseline corrected with a third-order polynomial, apodized with a Hamming window and zero filled. After two-dimensional Fourier transformation, the absolute value spectra were calculated. The τ value used for each measurements are specified in the figure captions.

2.9 EPR spectral simulations. All spectra were simulated using the EasySpin[15] package running in Matlab.

3. Results and Discussion

H-ZSM-5 samples were exchanged with CuCl through a dry process by direct sublimation of CuCl onto the zeolite at 573 K. Cu^+ ions were subsequently oxidised to Cu^{2+} with molecular oxygen at 348 K [9, **Errore. Il segnalibro non è definito.**10, 14]. Two samples are discussed in the following: sample one, where the framework oxide ions have been selectively labelled with ^{17}O, is referred to as Cu-^{17}**O**ZSM-5-$H_2{}^{16}O$, whereas sample two, where the solvating water molecules have been selectively labelled with ^{17}O, is hereafter denoted as Cu-^{16}OZSM-5-$H_2{}^{17}$**O**.

3.1 Continuous-wave (CW) EPR spectroscopy. The EPR spectrum of Cu-^{17}**O**ZSM-5-$H_2{}^{16}O$ was recorded both at 77K and room temperature (298 K) to assess the number of species present and the effect of thermal motion on their spectroscopic parameters.

At 77K the EPR spectrum is well-defined and the low-field region shows four clear features due to the hyperfine coupling between the electron spin and the $^{63,65}Cu$ nuclear spin (both I = 3/2). The hyperfine lines progressively broaden from low- (m_I = -3/2) to high-field (m_I = 3/2), such spectral broadening is associated to strain in g and A values, which stem from heterogeneity in the structural micro-environments of the Cu^{2+} centres and is commonly observed in Cu-loaded zeolites.[16] The EPR linewidth does not significantly differ from those measured in an analogue sample without ^{17}O framework enrichment, this is due to the non-quantitative substitution of all framework oxygen ions.

At 298 K, the EPR spectrum is broader, poorly defined especially in the low-field region and with an apparently reduced g anisotropy, as shown in Figure 2. This is consistent with anisotropy averaging mediated by molecular motion. Closer inspection reveals that faint traces of Cu^{2+} hyperfine lines are still visible between 260 and 330 mT, implying that at least a fraction of Cu^{2+} ions are immobile on the time scale of the EPR experiment.

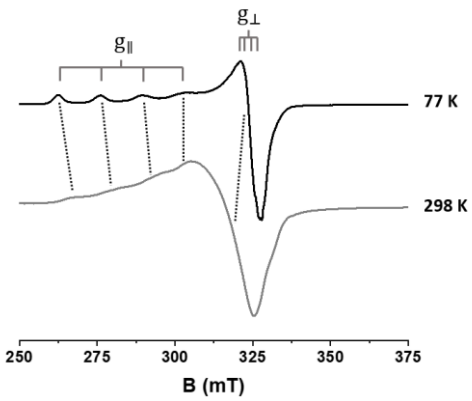

Figure 2. X-band CW-EPR spectra of Cu-^{17}**O**ZSM-5-$H_2{}^{16}O$ recorded at 77 K (black line) and at 298 K (grey line). Dotted lines mark the reduction in the ^{63,65}Cu hyperfine lines along $\mathbf{g}_{\parallel}$ as well as the shift in $\mathbf{g}_{\perp}$ observed between 77 and 298 K.

To quantitatively account for all these qualitative observations, the spectra were simulated to extract the spin-Hamiltonian parameters considering a single species at 77 K and two distinct species at 298 K, one rigid and one mobile. For the latter a characteristic correlation time of 2.5 x 10^{-10} s can be estimated (see Supporting Information Figure S1). Spectra simulations reveal that in all cases $g_{\parallel} > g_{\perp} > g_{\mathbf{e}}$ and $A_{\parallel} >> A_{\perp}$ implying a Singly Occupied Molecular Orbital (SOMO) mostly comprised of the d_{x2-y2} Cu^{2+} orbital.

	$g_{\parallel}$	$g_{\perp}$	$A_{\parallel}$	$A_{\perp}$	**Correlation time**	**Weight**
298 K						
Mobile species	2.40 ± 0.03	2.08 ± 0.02	360 ± 40	80 ± 20	2.5 x 10^{-10}± 0.6 x 10^{-10}	60%
Rigid species	2.345 ± 0.005	2.09 ± 0.01	444 ± 40	20 ± 5	/	40%
77K						
Rigid species	2.386 ± 0.002	2.079 ± 0.002	444 ± 10	20 ± 5	/	100%

Table 1. Spin Hamiltonian parameters extracted from simulation of hydrated Cu-ZSM5 at room temperature. All hyperfine interactions are given in units of MHz, whereas the correlation time is given in unit of s.

The CW EPR spectrum of Cu-^{16}OZSM-5-$H_2{}^{17}$**O** displays identical **g** tensor values and ^{63,65}Cu hyperfine couplings but much larger linewidth as a consequence of ^{17}O hyperfine couplings (see Supporting Information Figure S2 and S3).

3.2 ENDOR and HYSCORE spectroscopies. The EPR spectrum of a powder sample represents the envelope of all possible Cu^{2+} spin orientation with respect to the applied magnetic field. Hence for a fixed magnetic field value only certain orientations are on resonance and contribute to the measured ENDOR and HYSCORE spectra, see Figure 3 for a depiction of the set of orientations brought on resonance at selected field positions. This orientation-selectivity can in turn be exploited to measure the hyperfine components in the frame of the **g** tensor and provide structural constraints useful to outline the molecular structure for the Cu^{2+} ions bound to the zeolite framework.

The ENDOR spectra for both samples show structured signal in the range 1-60 MHz, Figure 3. The high-field region (45-60 MHz) is attributed to ^{1}H, whereas ^{17}O resonances span the whole low-field region (1-45 MHz). All ENDOR signals show a clear field-dependence which stems from the anisotropy of the hyperfine tensor. Representative HYSCORE spectra are reported in the Supporting Information Figure S4.

3.3 ^{17}O hyperfine couplings. Figure 3a reports the ENDOR spectra for the Cu-^{16}OZSM-5-$H_2{}^{17}$**O** sample across the EPR envelope recorded at 10 K. The ^{17}O-ENDOR versus field pattern is dominated by the anisotropic ^{17}O

hyperfine interaction. The spectrum at $\boldsymbol{g}_{\parallel}$ (995 mT) is single-crystal like with hyperfine peaks only arising from those ions for which the external field lies along the $\mathbf{g}_{\parallel}$ axis. The doublet is centered at 20 MHz and separated by $2\nu_{17O}$ according to the strong coupling regime resonance condition $\nu_{ENDOR} = A/2 \pm \nu_{17O}$ (see Experimental section), corresponding to a coupling of ≈ 40 MHz. As the field is increased (i.e. g decreases), this signal shifts at higher frequency, becomes broader and splits into two branches. This is due to the contribution of different spin orientation at intermediate *g* values. Despite the very high signal-to-noise ratio of the spectra, no signal belonging to weakly coupled ($\nu_{ENDOR} = \pm A/2$, with $\nu_{17O} \approx 6$ MHz) ^{17}O nuclei could be detected.

Figure 3b displays the ENDOR spectra for Cu-^{17}**O**ZSM-5-$H_2{}^{16}$O recorded at 10 K. The field-dependent spectra show a trend closely resembling that reported on Cu-^{16}OZSM-5-$H_2{}^{17}$**O** for in Figure 3a, with two relatively narrow peaks at $g_{\parallel}$ centred at $A/2$ = 22 MHz, which broaden and move to larger hyperfine couplings as moving towards $g_{\perp}$. The ENDOR effect for this sample is weaker due to the statistical nature of the isotopic enrichment which allows to substitute around 70% of the Si-O-Al oxide ions.[13] However, the presence of clear ^{17}O signal for the Cu-^{17}**O**ZSM-5-$H_2{}^{16}$O definitively demonstrates that even in presence of water Cu^{2+} ions are not completely solvated, but remain bound to the (isotopically enriched) framework.

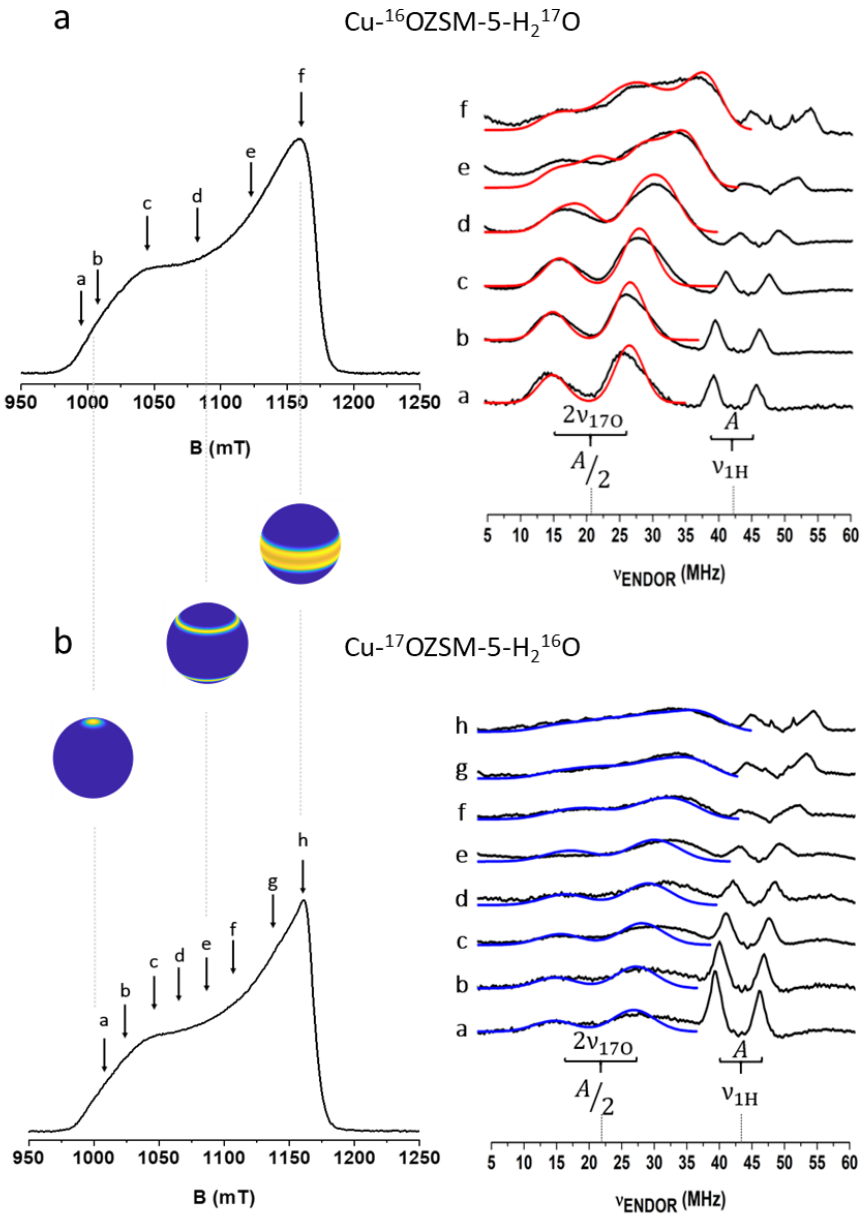

Figure 3. Q-band echo-detected EPR spectra and Q-band Davies ENDOR spectra obtained at different field positions across the EPR envelope of (a) Cu-^{16}OZSM-5-H_2**^{17}O** and (b) Cu-**^{17}O**ZSM-5-$H_2{}^{16}$O. The orientation selection effect due to g anisotropy is shown (in yellow) on unit spheres at selected field positions across the EPR envelope. Experimental spectra are reported in black while simulations are reported either as red or blue lines. The experimental ENDOR spectra in (b) were baseline corrected with a third-order polynomial function. The linewidth for the ENDOR simulations was set to 5 MHz (a) and 7 MHz (b). All spectra were recorded at 10 K.

Both sets of ENDOR spectra can be satisfactorily accounted for by a single oxygen species implying that, the coordination environment of Cu^{2+} in ZSM-5 has a high symmetry. For each sample, all ENDOR spectra were simulated at once in order to improve the reliability of the fitting. The derived hyperfine tensors have axial symmetry and their unique component $A_{\parallel}$ is orthogonal (θ = 90°) to $g_{\parallel}$. In turn this geometrical relationship is a clear indication of an equatorial coordination of both zeolite framework oxide ions and solvating water molecules. Furthermore, all hyperfine tensors are dominated by the isotropic contribution denoting a non-negligible degree of covalency between Cu^{2+} and both framework and water oxygen donor atoms. All simulation parameters are summarised in Table 2.

It is often assumed that Cu^{2+} ions in hydrated zeolites may detach from the framework to produce the aquo-complex ($[Cu(H_2{}^{17}O)_6]^{2+}$) [17], it is therefore useful to take this complex as a point of reference. ^{17}O hyperfine couplings for $[Cu(H_2{}^{17}O)_6]^{2+}$ have been reported by different research groups. Getz and Silver [18] detected two sets of hyperfine coupling tensors attributed to the nearest and the farthest equatorial waters and characterized by the largest principal value in the range 45-50 MHz. The existence of two distinct hyperfine tensors was interpreted as a consequence of a slightly distorted coordination geometry. Cox *et al.* [19] confirmed these findings but also detected an unresolved peak centered at the ^{17}O Larmor frequency which was attributed to axially coordinated water. In the case of Cu-ZSM-5 the measured hyperfine couplings are in line with the literature values for ^{17}O the equatorial position with a Cu-O distance in the range 0.228 - 0.231 nm[20,21], but no sign of weakly coupled ^{17}O nuclei could be detected through ENDOR spectroscopy. In an effort to identify axial ligands, HYSCORE experiments were performed on the Cu-^{16}OZSM-5-H_2**^{17}O** sample and are reported in Supplementary Information Figure S4. ^{17}O HYSCORE yielded a weak signal with a maximum coupling of ≈ 1.5 MHz, significantly lower than the reported values[22]. The lack of characteristic hyperfine coupling constants suggests either a square pyramidal coordination (where the bond length of fifth, apical ligand is longer than usual) or square planar geometry. A ^{27}Al hyperfine coupling is also detectable through HYSCORE spectroscopy (see Supporting Information Figure S5) and yields a coupling constant of ≈ 3 MHz, which is in line with previously reported values for similar systems [23,24,25], and confirms that the Cu^{2+} binds to a Brønsted site.

Analysis of the isotropic contact term and of the dipolar component *T* for the large hyperfine couplings obtained through ENDOR spectroscopy allows to evaluate the spin density on the oxygen orbitals and to provide a direct estimate of the degree of covalency of the Cu-O bond. For Cu-**^{17}O**ZSM-5-$H_2{}^{16}$O, by introducing the atomic value A^0 = -4622.8 MHz [26] for the isotropic hyperfine constant in the formula $\rho_s = a_{iso}/A^0$, the spin density on the *2s* orbital is calculated to be ρ_s = 0.011. In a similar fashion, the $2p_z$ spin density is calculated according to $\rho_p = T^p/T^0$, where T^0 is the atomic value for the dipolar hyperfine constant T^0 = 130.4 MHz [26]. However, the experimental *T* value also contains a through-space purely dipolar contribution (T^d) between the spin population on the Cu nucleus and the ^{17}O magnetic moment, which does not depend on the nature of the Cu-O bond but only on the spatial distance between the two nuclei. Assuming a Cu spin population of 70 % and a (lower bound) Cu-O distance of 0.2 nm, T^d can be estimated to be T^d = [1.10, 1.10, -2.20] MHz. Hence, the proper value for T^p, calculated as $T^p = T - T^d$ = 8.00 - 1.10 MHz = 6.90 MHz, yields a ρ_p = 0.051. The total spin density on the framework oxide ion in Cu-**^{17}O**ZSM-5-$H_2{}^{16}$O is thus $\rho = \rho_s + \rho_p$ = 0.062. In other words, each framework oxygen ion has a 6% total participation to the SOMO. Given the similarities in the hyperfine values the solvating water oxygen (Cu-^{16}OZSM-5-H_2**^{17}O**)

contribute to a similar extent. Interestingly these values are slightly higher than those reported for $[Cu(H_2{}^{17}O)_6]^{2+}$ complexes which amount to a 4-6% participation for a single equatorial ^{17}O atom [19], and with the computed value (3.35%) reported for non-isotopically enriched $[Cu(H_2O)_5]^{2+}$ [27]. A similar value was found in $Cu(acac)_2$ complex, where the calculated participation of oxygen atomic orbitals is ≈ 6% [28, 29]. Thus, even for alike equatorial positions, the Cu-O bond in Cu-ZSM-5 affords a higher degree of covalency than $[Cu(H_2O)_6]^{2+}$ and thus a shorter bond length, further proving that Cu^{2+} maintain strong interactions with the zeolite framework even in presence of solvating water.

The ENDOR spectra show no resolved features due to the quadrupole interaction, this may stem from broadening as a result of structural heterogeneity similar to the effect observed in the CW EPR spectra (see Figure 1). However, from the ENDOR linewidth (5 MHz and 7 MHz) it is possible to estimate un upper limit for the nuclear quadrupole coupling of 0.42 and 0.58 MHz for Cu-^{17}**O**ZSM-5-$H_2{}^{16}O$ and Cu-^{16}OZSM-5-$H_2{}^{17}$**O** respectively, according to the relationship ENDOR linewidth ≈ 12 times the orientation dependent quadrupole coupling[30].

3.4 ^{1}H Hyperfine Couplings. Further evidence of the coordination geometry and of the network of solvating water molecules around the Cu^{2+} centre can be derived from ^{1}H hyperfine couplings. The ^{1}H region of the Davies-ENDOR spectra reported in Figure 3 is virtually identical for both samples, however a higher resolution is achieved with the Mims ENDOR pulse sequence and Figure 4 reports the experimental data for Cu-^{16}OZSM-5-$H_2{}^{17}$**O** obtained at field positions corresponding to $g_\parallel$ and $g_\perp$. The spectra can be simulated by considering two classes of ^{1}H nuclei, H1 responsible for the outer part of the spectrum (large coupling) and H2 responsible for the inner part of the spectrum (small coupling), the hyperfine values are reported in Table 2.

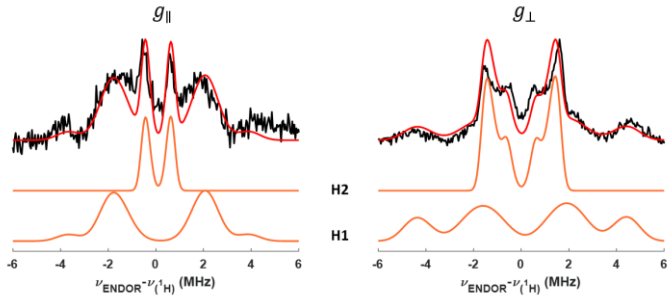

Figure 4. Q-band Mims ENDOR spectra obtained for Cu-^{16}OZSM-5-$H_2{}^{17}$**O** at the field positions corresponding to $g_\parallel$ and $g_\perp$, as indicated in the figure. The experimental spectra are reported as black lines, the best simulations are reported in red whereas individual contribution for H1 and H2 are reported in orange. The *x*-axis frequency scale reports the offset from the ^{1}H Larmor frequency (ν_H) at each field position. All spectra were recorded at 10 K.

The analysis of the H1 hyperfine tensor leads to extract the isotropic contact term a_{iso}= -1.3 MHz and a rhombic dipolar tensor T = [-8.0, -3.0, 11.0] MHz. These coupling values reproduce both the rhombicity and the magnitude observed for water molecules directly bound to a Cu^{2+} ion in the equatorial position in a $[Cu(H_2O)_6]^{2+}$ complex [20] (average values, a_{iso}= -0.87 MHz and T = [-7.12, -3.21, 10.33] MHz) and can therefore be confidently assigned to ^{1}H nuclei belonging to an equatorial water. The larger a_{iso} for H1 measured in Cu-^{16}OZSM-5-$H_2{}^{17}$**O** strengthens the conclusion that the Cu-O bond length is shorter than that measured in $[Cu(H_2O)_6]^{2+}$.

Similar analysis conducted on H2 hyperfine tensor yields an almost purely dipolar hyperfine coupling with a_{iso}= 0.17 MHz and an axial dipolar tensor T = [-1.57, -1.57, 3.13] MHz. These hyperfine values are smaller than those expected for an axial water, whose average values have been reported to be a_{iso}= 0.145 MHz and T = [-3.54, -3.84, 7.38] MHz [20].

From the experimental dipolar tensor it is possible to calculate the distance between the Cu(II) spin and the ^{1}H nuclear spin of H2. Considering the point dipole approximation, the dipolar component of the hyperfine tensor takes the form

$$T = \frac{\mu_0}{4\pi} g_e g_n \beta_e \beta_n \frac{1}{r^3} \qquad \text{(Eq.1)}$$

where all constants have their usual meaning and *r* is the distance between the electron spin on Cu and H2. Eq. 1 yields a Cu-H2 distances $r_{Cu\text{-}H2}$ = 0.368 nm which is considerably longer than the expected distance for an axially coordinated water molecule, further confirming that axial ligands, if at all present, are only loosely bound to the Cu ion. Alternatively, this data suggests that a water molecule is tightly bound in the second coordination sphere.

Species	a_{iso}	T_1	T_2	T_3	**[α,β,γ]**
H1-water (equatorial)	-1.3 ± 0.1	-8.0 ± 0.5	-3.0 ± 0.5	11.0 ± 0.6	[0,90,50] ±10
H2-water (distal)	0.17 ± 0.02	-1.57 ± 0.05	-1.57 ± 0.05	3.13 ± 0.05	[0,90,0] ±10
^{17}O-water	-50.0 ± 0.5	8.0 ± 1.0	8.0 ± 1.0	-16.0 ± 1.0	[0,90,0] ±10
^{17}O-framework	-51.0 ± 0.5	7.0 ± 1.0	7.0 ± 1.0	-14.0 ± 1.0	[0,90,0] ±10

Table 2. Hyperfine coupling constants extracted from experimental ENDOR spectra. All hyperfine interactions are given in units of MHz, while the Euler angles [α,β,γ] are in degrees. The negative sign of the a_{iso} value was assumed based on the negative g_n value of ^{17}O and in line with literature reports [18,19,2222].

3.5 Cu-ZSM-5 structural model. The spectroscopic results presented can be summarised as follows: (i) the Cu^{2+} ions bind simultaneously to the zeolite framework and to solvating water molecules; (ii) the overall symmetry of this interfacial complex is high considered that only one hyperfine tensor accounts for all framework oxide ions or solvating water molecules; and (iii) the estimated Cu-H distances can be used to further refine the structure and suggest a water molecule in the second coordination sphere. Figure 5 reports a structural model compatible with the ^{17}O and ^{1}H spectroscopic constraints. The overall geometry can be interpreted as square planar with a slight asymmetry between framework and water oxygen nuclei. Although it is not possible to unambiguously determine the number of equivalent oxygen ions from ^{17}O-ENDOR, the absence of ^{17}O signals due to weakly coupled oxygen nuclei in the HYSCORE spectra suggests that the axial position stays vacant, and is therefore not represented in Figure 5.

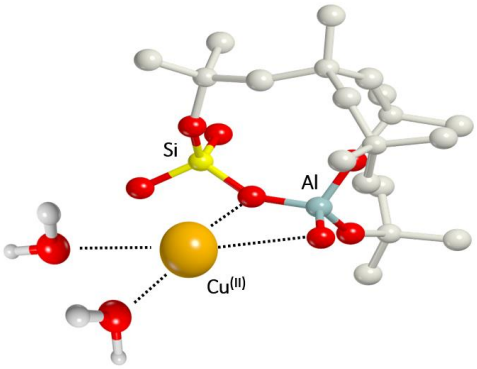

Figure 5. Structural model for single-ion Cu^{2+} in hydrated ZSM-5 as derived from EPR data. The overall coordination geometry is square planar. An additional water molecule is likely present in the second coordination sphere, but not shown since the exact position could not be determined from EPR data. For clarity, only a portion of the ZSM-5 framework is shown. Colour code: Yellow: Silicon; Grey: Aluminium; Orange: Copper; Red: Oxygen; White: Hydrogen.

***3.6 S* = 1/2 ions supported on ZSM-5.** An understating of the bonding interaction between metal and zeolite support can be achieved by comparing the EPR spectroscopic observables **g** and **A** tensors which allow to determine the nature of the SOMO orbital. For the series of S = ½ metals VO^{2+} $(3d^1)$[10], Cu^{2+} $(3d^9)$ and Zn^+ $(3d^{10}4s^1)$[13] supported on ZSM-5, based on the measured g factors and considering simple crystal field arguments the metal orbital hosting the unpaired electron is determined to be $3d_{xy}$, $3d_{x2-y2}$ and $4s$ respectively, which represents the dominant contribution to the SOMO orbital, see Figure 6.

In turn, the different nature of the SOMO orbital explains why the measured hyperfine coupling for Cu^{2+} and Zn^+ is one order of magnitude larger than VO^{2+}. The SOMO of VO^{2+} is a non-bonding d_{xy} orbital, whereas the unpaired electron occupies a d_{x2-y2} and a s anti-bonding orbital in Cu^{2+} and Zn^+, respectively. This difference can be pictured graphically considering that the d_{x2-y2} and d_{xy} orbitals are related by a 45° rotation about the z axis, which is assumed coincident with the $g_{\|}$ axis. While the d_{x2-y2} orbital points directly towards the oxygen ligands, the d_{xy} points between them resulting in non-bonding molecular orbital, as can be seen in Figure 6. The spherical symmetry (s character) of the Zn^+ SOMO makes it the least sensitive to such geometrical considerations and allows a high degree of overlap with the oxygen orbitals. As a result, both Zn^+ [13] and Cu^{2+} display an ≈ 6-8% electron spin density on the oxygen valence orbital, whereas the percentage drops to 2% in the case of VO^{2+} [10]. A similar trend is observed in the ^{14}N hyperfine couplings of the popular porphyrin and phthalocyanine metal complexes, where VO^{2+} yields an a_{iso} coupling of ≈ 6 MHz [31,32] and Cu^{2+} of ≈ 50 MHz [33]. Given that for ^{14}N A^0_{14N} = 1540 MHz [26], the isotropic hyperfine couplings translate into $\rho^s_{VO^{2+}}$ ≈ 0.4% and $\rho^s_{Cu^{2+}}$ ≈ 3%. The much larger ρ^s contribution for ^{14}N as compared to ^{17}O is a consequence of the sp^3 hybridisation of O in water and zeolite and sp^2 for N in porphyrin/phtalocyanine. In view of all of the above, it can be concluded that while the spin density transfer of Cu^{2+} and Zn^+ stems from a sigma-bonding interaction, the transfer is essentially entirely due to pi-bonding interaction in the case of VO^{2+}.

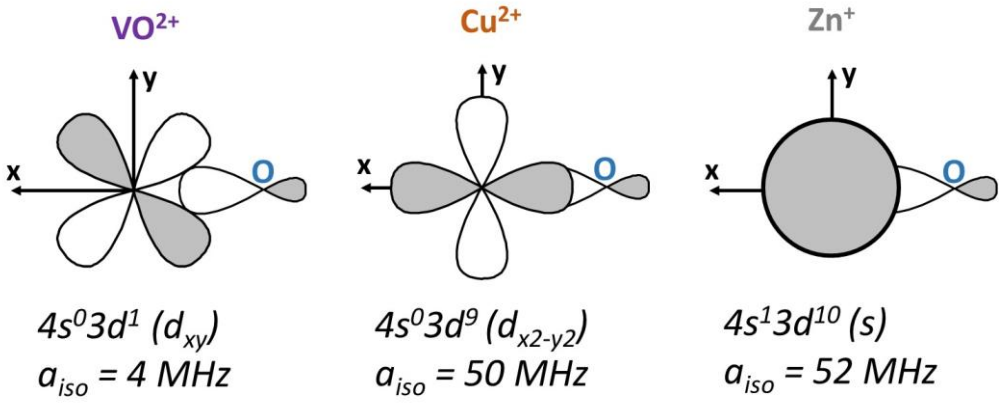

Figure 6. Schematic representation (top view) of the orbital interaction of VO^{2+}, Cu^{2+} and Zn^+ and a sp^3 oxide ion in ZSM-5. The corresponding electronic configuration, the metal orbital with main contribution to the SOMO and the ^{17}O isotropic hyperfine coupling constants are also reported (VO^{2+} and Zn^+ hyperfine parameters are derived from refs. 10,13). For clarity, only one oxide ligand is depicted.

4. Conclusions

The combined analysis of ^{17}O hyperfine coupling due to zeolite framework oxide ions as well as ^1H and ^{17}O hyperfine couplings from solvating water allowed to establish a square planar coordination geometry for single-site Cu ions in ZSM-5 zeolite and that the Cu^{2+} ions maintain an intimate contact with the framework even in presence of solvating water. This is noteworthy since the coordination geometry for Cu^{2+} in ZSM-5

is often reported as octahedral and the Cu^{2+} ions are believed to fully detach from the framework in presence of solvating molecules (e.g. H_2O and NH_3). The exquisite advantage of EPR hyperfine techniques as compared to other spectroscopies (e.g. EXAFS and XANES) is that they are selective towards paramagnetic species and that each ligand may be selectively labelled and its contribution to the electronic structure independently assessed. This allows to reach structural definition at atomic resolution even for large and non-crystalline samples, which is a prerequisite for the description and understanding of structure-function relationships.

The comparison of the data presented here for Cu^{2+}-^{17}O hyperfine couplings with VO^{2+}-^{17}O and Zn^{+}-^{17}O all bound to the same zeolite ZSM-5 framework allow to rationalise the binding mode and the factors dictating the degree of covalency. This further proves that the zeolite framework does not behave as a simple inert support but rather as a macroligand and allow to draw analogies between classical and interfacial coordination chemistry.

Associated Contents

Supporting information

CW-EPR spectra and their simulations, HYSCORE spectra

Author Information

Corresponding Author

*E-mail: enrico.salvadori@unito.it

Notes

The authors declare no conflict of interests.

Acknowledgement

The Authors gratefully acknowledge Mrs Valeria Lagostina for help in sample preparation.

References

(1) Wang, A.; Li, J.; Zhang, T. Heterogeneous single-atom catalysis. *Nat. Rev. Chem.* **2018***, 2*, 65–81.

(2) Paolucci, C.; Di Iorio, J. R.; Schneider**,** W. F.; Gounder**,** R. Solvation and Mobilization of Copper Active Sites in Zeolites by Ammonia: Consequences for the Catalytic Reduction of Nitrogen Oxides. *Acc. Chem. Res.* **2020**, *53* (9), 1881–1892.

(3) Parvulescu, V. I.; Grange, P.; Delmon, B. Catalytic removal of NO. *Catal. Today* **1998**, *46*, 233−316.

(4) Mohan, S.; Dinesha, P.; Kumar, S. NOx reduction behaviour in copper zeolite catalysts for ammonia SCR systems: A review. *Chem. Eng. J.* **2020**, *384*, 123253.

(5) Sushkevich**,** V. L.; van Bokhoven**,** J. A. Methane-to-Methanol: Activity Descriptors in Copper-Exchanged Zeolites for the Rational Design of Materials. *ACS Catal.* **2019**, *9* (7), 6293–6304.

(6) Lin, L.; Fan, M.; Sheveleva, A.M.; Han X.; Tang Z.; Carter J.H.; da Silva I.; Parlett C.M.A.; Tuna F.; McInnes E.J.L.; Sastre G.; Rudić S.; Cavaye H.; Parker S.F.; Cheng Y.; Daemen L.L.; Ramirez-Cuesta A.J., Attfield M.P.; Liu Y.; Tang C.C.;

Han B.; Yang S. Control of zeolite microenvironment for propene synthesis from methanol. *Nat Commun* **2021**, *12*, 822.

(7) Turnes Palomino, G.; Fisicaro, P.; Bordiga, S.; Zecchina, A.; Giamello, E.; Lamberti, C. Oxidation States of Copper Ions in ZSM-5 Zeolites. A Multitechnique Investigation. *J. Phys. Chem. B* **2000**, *104* (17), 4064-4073.

(8) Godiksen, A.; Vennestrøm, P. N. R.; Rasmussen, S. B.; Mossin, S. Identification and Quantification of Copper Sites in Zeolites by Electron Paramagnetic Resonance Spectroscopy. *Topics in Catalysis* **2017**, *60* ,13–29.

(9) Spoto, G.; Zecchina, A.; Bordiga, S.; Ricchiardi, G.; Martra, G.; Leofanti, G.; Petrini, G. Cu(I)-ZSM-5 zeolites prepared by reaction of H-ZSM-5 with gaseous CuCl: Spectroscopic characterization and reactivity towards carbon monoxide and nitric oxide. *Appl. Cat. B: Env.* **1994**, *3*(2–3), 151-172.

(10) Lagostina, V.; Salvadori, E.; Chiesa, M.; Giamello, E. Electron paramagnetic resonance study of vanadium exchanged H-ZSM5 prepared by vapor reaction of VCl_4. The role of ^{17}O isotope labelling in the characterisation of the metal oxide interaction. *J. Catal.* **2020**, *391*, 397-403.

(11) Harmer, J. R. Hyperfine Spectroscopy – ENDOR. *eMagRes* **2016**, *5*, 1493–1514.

(12) Van Doorslaer, S. Hyperfine Spectroscopy: ESEEM. *eMagRes* **2017**, *6*, 51–70.

(13) Morra, E.; Signorile, M.; Salvadori, E.; Bordiga, S.; Giamello, E.; Chiesa, M. Nature and Topology of Metal–Oxygen Binding Sites in Zeolite Materials: ^{17}O High-Resolution EPR Spectroscopy of Metal-Loaded ZSM-5. *Angew. Chem. Int. Ed.* **2019**, *58*, 12398.

(14) Spoto, G.; Bordiga, S.; Scarano, D.; Zecchina A. Well defined Cu(I)(NO), $Cu(I)(NO)_2$ and Cu(II)(NO)x (X=O- and/or NO2-) complexes in Cu(I)-ZSM5 prepared by interactions of H-ZSM5 with gaseous CuCl. *Cat. Lett.* **1992**, *13*, 39-44.

(15) Stoll, S.; Schweiger, A. EasySpin, a comprehensive software package for spectral simulation and analysis in EPR. *J. Magn. Reson.* **2006**, *178* (1), 42-55.

(16) Carl, P. J.; Larsen, S. C. EPR Study of Copper-Exchanged Zeolites: Effects of Correlated *g*- and *A*-Strain, Si/Al Ratio, and Parent Zeolite. *J. Phys. Chem. B* **2000**, *104* (28) 6568–6575.

(17) Giordanino, F.; Vennestrøm, P. N.; Lundegaard, L. F.; Stappen, F. N.; Mossin, S.; Beato, P.; Bordiga, S.; Lamberti, C. Characterization of Cu-exchanged SSZ-13: a comparative FTIR, UV-Vis, and EPR study with Cu-ZSM-5 and Cu-β with similar Si/Al and Cu/Al ratios. *Dalt. Trans.* **2013**, *42*, 12741-12761.

(18) Getz, D., Silver, B. L., ESR of $Cu^{2+}(H_2O)_6$. I. The oxygen-17 superhyperfine tensors in $^{63}Cu^{2+}$ doped zinc Tutton's salt at 20°K. *J. Chem. Phys.* **1974**, *61* (2), 630-637.

(19) Cox, N., Lubitz, W., Savitsky, A. W-band ELDOR-detected NMR (EDNMR) spectroscopy as a versatile technique for the characterisation of transition metal–ligand interactions. *Mol. Phys*. **2013**, *111*, 2788-2808.

(20) Atherton, N. M., Horsewill, A. J., Proton ENDOR of $Cu(H_2O)_6^{2+}$ in $Mg(NH_4)_2(SO_2)_4 \bullet 6H_2O$. *Mol. Phys.* **1979**, 37 (5) 1349-1361.

(21) Colaneri, M. J.; Teat, S. J.; Vitali, J. Electron Paramagnetic Resonance Characteristics and Crystal Structure of a Tutton Salt Analogue: Copper-Doped Cadmium Creatininium Sulfate. *J. Phys. Chem. A* **2020**, *124* (11), 2242–2252.

(22) Colaneri, M. J.; Vitali, J. Probing Axial Water Bound to Copper in Tutton Salt Using Single Crystal ^{17}O-ESEEM Spectroscopy. *J. Phys. Chem. A* **2018**, *122* (30), 6214–6224.

(23) Goldfarb, D.; Kevan, L. ^{27}Al fourier-transform electron-spin-echo modulation of Cu^{2+}-doped zeolites A and X. *J. Mag. Res.* **1989**, *82* (2) 270-289.

(24) Goldfarb, D.; Zukerman, K. Characterization of Cu^{2+} sites in zeolites NaX and KX by ^{27}Al electron spin echo envelope modulation. *Chem. Phys. Lett.* **1990**, *171* (3), 167-174.

(25) Carl, P. J.; Vaughan, D. E. W.; Goldfarb, D. Interactions of Cu(II) Ions with Framework Al in High Si:Al Zeolite Y as Determined from X- and W-Band Pulsed EPR/ENDOR Spectroscopies. *J. Phys. Chem. B* **2002**, *106* (21), 5428–5437.

(26) Fitzpatrick, J. A. J.; Manby, F. R.; Western, C. M., The Interpretation of Molecular Magnetic Hyperfine Interactions. *J. Chem. Phys.* **2005**, *122*.

(27) Frank, P., Benfatto, P., Szilagyi, R., D'Angelo, P., Della Longa, S., Hodgson, K. The Solution Structure of $[Cu(aq)]^{2+}$ and Its Implications for Rack-Induced Bonding in Blue Copper Protein Active Sites. *Inorg. Chem* **2005**, *44* (6) 1922-1933.

(28) de Almeida, K. J., Ramalho, T.C., Rinkevicius, Z., Vahtras, O., Ågren, H., Cesar, A. Theoretical Study of Specific Solvent Effects on the Optical and Magnetic Properties of Copper(II) Acetylacetonate. *J. Phys. Chem. A* **2011**, *115* (8), 1331–1339.

(29) de Almeida, K. J., Cesar, A., Rinkevicius, Z., Vahtras, O., Ågren, H. Modelling the Visible Absorption Spectra of Copper(II) Acetylacetonate by Density Functional Theory. *Chem. Phys. Lett*. **2010**, *492*, 14-18.

(30) Carepo, M.; Tierney, D. L.; Brondino, C. D.; Yang, T. C.; Pamplona, A.; Telser, J.; Moura, I.; Moura, J. J. G.; Hoffman, B. M. ^{17}O ENDOR Detection of a Solvent-Derived Ni−(OH_x)−Fe Bridge That Is Lost upon Activation of the Hydrogenase from *Desulfovibrio gigas. J. Am. Chem. Soc.* **2002**, *124* (2), 281–286.

(31) Moons, H.; Patel, H. H.; Gorun, S. M.; Van Doorslaer, S. Electron Paramagnetic Resonance and DFT Analysis of the Effects of Bulky Perfluoroalkyl Substituents on a Vanadyl Perfluoro Phthalocyanine. *Z. Phys. Chem.* **2017**, 231 (4), 887–903.

(32) Atzori, M.; Tesi, L.; Morra, E.; Chiesa, M.; Sorace, L.; Sessoli, R. Room-Temperature Quantum Coherence and Rabi Oscillations in Vanadyl Phthalocyanine: Toward Multifunctional Molecular Spin Qubits. *J. Am. Chem. Soc.* **2016**, *138* (7), 2154–2157.

(33) Finazzo, C.; Calle, C.; Stoll, S.; Van Doorslaer, S.; Schweiger, A. Matrix effects on copper(ii)phthalocyanine complexes. A combined continuous wave and pulse EPR and DFT study. *Phys. Chem. Chem. Phys.* **2006**, *8*, 1942-1953.